Compact Green Harmonic Transponders for Parcel Tracking

Leonardo Balocchi, Valentina Palazzi, *Member, IEEE*, Stefania Bonafoni, *Member, IEEE*, Federico Alimenti, *Senior Member, IEEE*, Paolo Mezzanotte, *Member, IEEE*, and Luca Roselli, *Fellow, IEEE*

***Abstract*—This article presents a harmonic transponder, designed to minimize the tag sensitivity to the materials close to it. The tag is based on a dual-frequency dual-port patch antenna and a frequency doubler. The tag is designed to be interrogated by the fundamental frequency f_0 equal to 2.4 GHz and it backscatters a signal at $2f_0 = 4.8$ GHz. The patch is realized on cardboard, while the frequency doubler and the feedlines are manufactured on a flexible polylactic acid (PLA) substrate. The feed lines are electromagnetically coupled to the patch through H slot apertures. A complete prototype with an area occupation of 5 × 10 cm^2 was manufactured and directly integrated in a parcel. The antenna features a front-to-back ratio higher than 12 dB at both operating frequencies. The tag could be read up to a distance of 6 m with a transmitted power of 25 dBm Equivalent Isotropically Radiated Power (EIRP), regardless of the object placed in the parcel close to the tag. This work opens the door to a new class of harmonic transponders for tracking applications, characterized by low environmental impact, high integrability, compactness and reliability, which can find application in many Internet of Things emerging applications.**

***Index Terms*—Harmonic RFID, antenna design, slot-fed dual-port patch antenna, green substrates.**

I. Introduction

STATE-OF-THE-ART non-optical systems for automatic goods tracking generally rely on Ultra High Frequency (UHF) Radio-Frequency Identification (RFID) transponder based on the Electronic Product Code (EPC) Gen2 standard. Generally, UHF RFID tags are based on dipole antennas that, due to their omnidirectional radiation pattern, are affected by the presence of objects (materials) inside the package, so their radiation pattern can be modified and their read range reduced, leading to the miss-detection of some packages. Additionally, UHF RFID systems can be affected by self-jamming (this is especially true for systems operating in highly cluttered environments), while the receiver sensitivity is usually impaired by the power leakage between the transmitted and the receiver and by the transmitter phase noise [1].

Studies were conducted to reduce the impact of metal and other materials on the RFID tags performance. Lach et al. [2] investigate the performance degradation of UHF-RFID tags considering the impact of objects and materials in its immediate proximity; in [3] the focus is on surface materials for the RFID placement, and it emphasises how materials used as packaging in logistics environments, combined with their contents, often result in a complex and inhomogeneous environment. Further analysis of the impact that metals in the environment have on the radiation pattern of the tag and thus on the overall characteristics of the antennas are described in [4] and [5]. Variations in performance for passive UHF RFID in practical conditions [6] lead back to a general problem of interaction with objects placed in the environment.

Harmonic tags can represent an effective alternative to RFID systems in such harsh application scenarios. Simple harmonic transponders have already been used to study the behavior of bees [7], or for avalanche victim rescue [8]. This is because harmonic systems are robust to clutter, and rely on simple circuit architectures.

A drawback of harmonic systems with respect to standard UHF RFID transponders is the need for transmitting and a receiving antennas working at different frequencies on the tag, which might lead to cumbersome transponders [9]. Solutions based on dual-frequency single antennas have been studied [10], [11]. However, these solutions are based on dipole antennas, and more generally on isotropic radiators. By interacting with the materials of the items where the tag is placed, antennas can be detuned, thereby impairing the reliability of the system.

In [12], the feasibility of a slot-fed dual-port rectangular patch antenna for harmonic transponders was presented, although the antennas were manufactured using standard substrates for radio-frequency (RF) applications. In particular, the antenna was demonstrated on standard materials, GML 1000 and RT/duroid 5880.

The extension presented in this new work consists of adapting the proposed structure to organic materials, i.e., cardboard and bioplastics, with the aim to ease the tag integration in parcels and packages. So, first the new substrate materials are characterized, and then the design is adapted to the new substrates. Additionally, a complete proof-of-concept transponder is manufactured and characterized. The harmonic tag was

Manuscript received 31 January 2023; revised 20 March 2023; accepted 21 March 2023. Date of publication 27 March 2023; date of current version 19 July 2023. This work was supported by the ECSEL Joint Undertaking (JU) under Agreement 101007247. The JU receives support from the European Union's Horizon 2020 Research and Innovation Programme and Finland, Germany, Ireland, Sweden, Italy, Austria, Iceland, Switzerland. *(Corresponding author: Leonardo Balocchi.)*

The authors are with the Department of Engineering, University of Perugia, 06125 Perugia, Italy (e-mail: leonardo.balocchi@studenti.unipg.it; valentina.palazzi@unipg.it; stefania.bonafoni@unipg.it; federico.alimenti@unipg.it; paolo.mezzanotte@unipg.it; luca.roselli@unipg.it).

Digital Object Identifier 10.1109/JRFID.2023.3262022

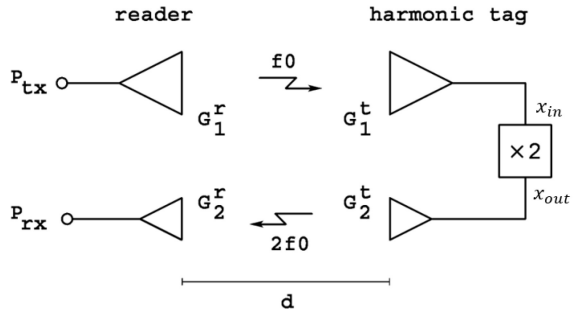

Fig. 1. Schematic diagram of the proposed harmonic system [12].

produced using the photolithography technique, and tested on a parcel, in proximity of metal and water.

II. System Overview

The block diagram of a generic harmonic system is shown in Figure 1. The system consists of a reader and a tag. The reader transmits a sinusoidal signal with a frequency f_0. This signal is captured by the input antenna of the tag and transmitted to the frequency doubler ("x_{in}" in Figure 1). The frequency doubler converts the signal into the second harmonic and it is usually based on a series-connected Schottky diode. The resulting output signal ("x_{out}" in Figure 1) is finally backscattered to the reader via the output antenna of the tag and it is detected by the receiver. The receiver is tuned to $2f_0$, which makes the system robust to environmental reflections and to the transmitter phase noise.

In this work a compact dual-port harmonic antenna system is proposed, which combines ease of manufacturing with robustness to detuning caused by metal/water. The tag is designed to be manufactured using low-cost and eco-friendly materials, including bioplastics and cardboard, to facilitate the tag integration in parcels and packages and to reduce their environmental impact. These materials feature significant limitations with respect to radio-frequency Printed Circuit Board (PCB) substrates: both cardboard and bioplastics cannot withstand high temperatures (polylactic acid, in particular, features a glass transition temperature of $60°C$), while cardboard has a high surface roughness and porosity. These limitations are taken into account in the circuit design and in the choice of the manufacturing technologies.

A. Materials Characterization

The dielectric materials adopted for the proof-of-concept tag prototype are polylactic (PLA) acid and cardboard. The thickness of the adopted PLA film is 300 μm, while the thickness of the cardboard is 2.5 mm. Both materials are electromagnetically characterized in the frequency range of interest using T resonators. The properties of the adopted PLA films were already reported in [13], corresponding to $\epsilon_r = 2.8$ and $\tan\delta = 0.008$. The results concerning cardboard characterization are reported in this section.

The T resonator is manufactured using the copper adhesive tape technology described in [14]. In particular, a piece of copper adhesive tape is shaped using photolithography and then stuck on the cardboard substrate using a sacrificial layer.

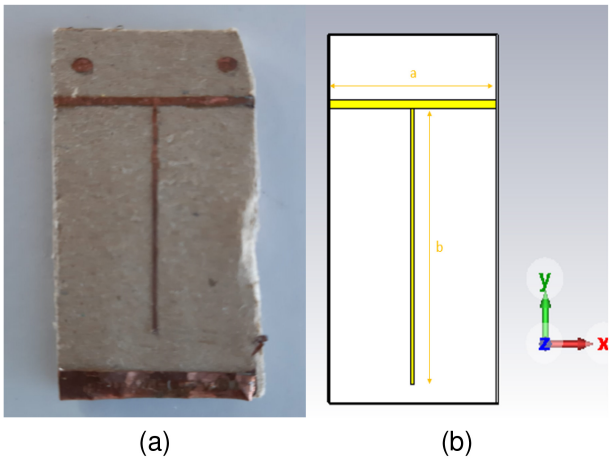

Fig. 2. (a) T-resonator on the cardboard. (b) Simulated T-resonator structure, $a = 20.4$ mm and $b = 30$ mm.

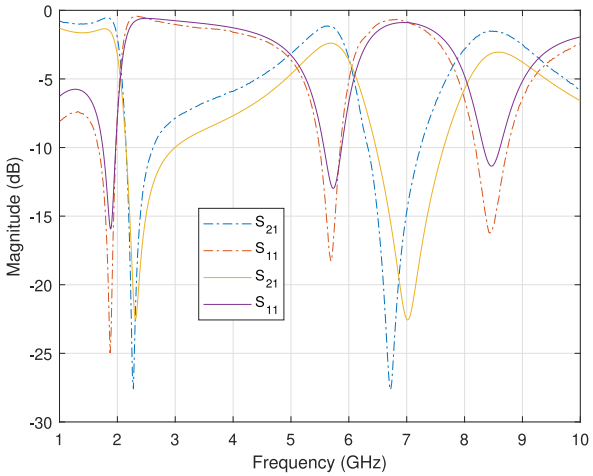

Fig. 3. Scattering parameters of the T resonator on cardboard. The solid lines correspond to simulated scattering parameters, and the dashed lines to the measured.

This way, cardboard is not involved in the wet chemical processes for copper etching. Additionally, we could combine high accuracy with a high quality factor (the metal traces are manufactured using bulk copper) [14], which improve the accuracy of the measurement.

A T resonator was therefore first applied over the substrate of interest (see Figure 2), the cardboard, and its scattering parameters (simulated and measured) were reported in Figure 3.

The ϵ_r and loss tangent of the cardboard material are found by matching the scattering parameters measured by connecting the prototype to the Vector Network Analyzer, with the scattering parameters of the T-resonator simulated with a full wave simulator (see Figure 3).

A good agreement is obtained for $\epsilon_r = 1.35$ and $\tan\delta = 0.02$.

III. Antenna Design

The antenna system designed for the tag consists of a dual-port slot-fed harmonic patch antenna, which is purposely developed to guarantee a compact layout for the tag, while

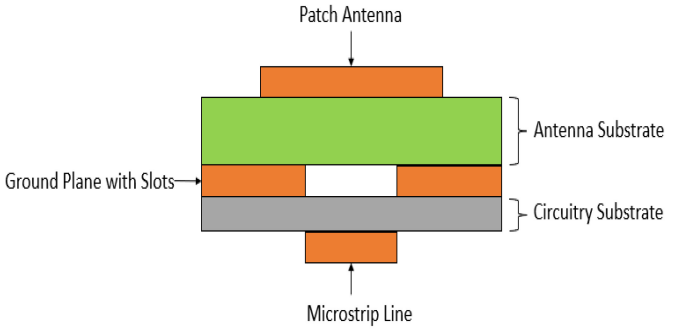

Fig. 4. Complete antenna with feature substrates, in green the 2.8 mm thick cardboard ($\epsilon_{r,cardboard} = 1.35$, $tan\delta_{cardboard} = 0.02$), and in grey the 0.3 mm thick PLA ($\epsilon_{r,PLA} = 2.54$, $tan\delta_{PLA} = 0.009$).

making it insensitive to the electromagnetic properties of the objects placed below it.

Figure 4 shows the antenna stackup, while Figure 5 shows the exploded view of the antenna layers with the main antenna dimensions. The antenna is designed to be matched to 50 Ω at both operating frequencies. One port is designed for the fundamental frequency $f_0 = 2.4$ GHz, and the other for the second harmonic $2f_0 = 4.8$ GHz

The harmonic antenna consists of a rectangular microstrip patch antenna which is fed with two orthogonal microstrip lines coupled with the patch through H-slots. The patch antenna is manufactured on cardboard (antenna substrate in Figure 2(a)), while the microstrip feed lines are manufactured on the PLA layer (circuitry substrate in Figure 2(a)). In this way, the antenna can benefit from a thick substrate, while the microstrip lines and the frequency doubler are realized on a thin substrate which guarantees lower radiation loss.

Figure 5(a) shows the rectangular patch: the long side of the patch resonates at f_0 (first resonance), while the short side resonates at $2f_0$. Therefore, the tag back-scatters the $2f_0$ signal in orthogonal polarization with respect to the received f_0 signal. Layer 2, in Figure 5(b), represents the ground plane for both the microstrip lines and the patch antenna, and hosts the slot apertures, two H-shaped slots, which allow electromagnetic coupling between the microstrip feed lines on the bottom layer and the patch on top layer. Thanks to this central metal layer, most of the antenna radiation is directed to the space above the patch, thereby reducing the tag sensitivity to the materials below it. Slot apertures were chosen instead of coaxial probes and other connection methods since they allow us to obtain a multi-layer antenna topology without requiring metalized vias through, which would represent a challenge from a manufacturing point of view. The total area occupation of the harmonic dual-frequency patch corresponds approximately to half the area of a square patch working at f_0.

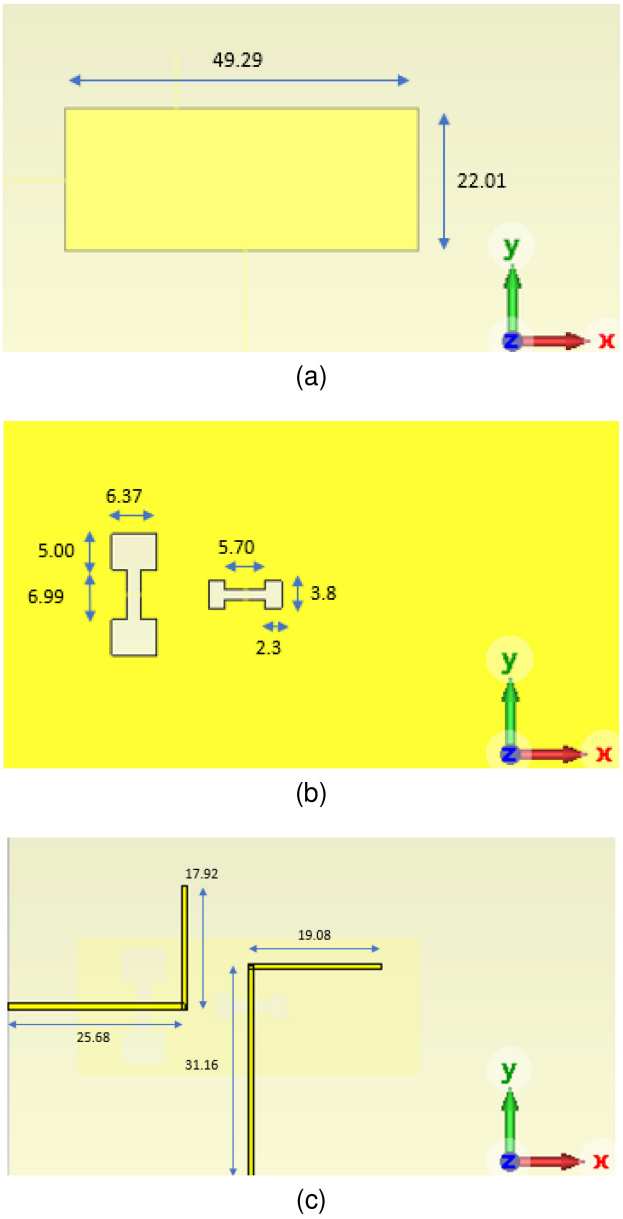

Fig. 5. Exploded view of the proposed antenna. (a) top layer, (b) ground plane and (c) bottom layer; the yellow colour represents the conductive pattern and the dimensions are expressed in mm.

A. Antenna Prototype

The metal traces corresponding to the three layers illustrated in Figure 5 are manufactured using the copper tape technology adopted for the T resonator. The mictostrip and ground layers are attached to the two sides of the PLA substrate; the patch antenna is attached to the cardboard. Then, the two substrates are aligned thanks to alignment marks and are attached using a simple stick glue. Due to the almost negligible thickness of the glue with respect to the cardboard, the impact of the stick glue is not modeled (it is part of the manufacturing tolerance). The top and bottom views of the antenna proof-of-concept prototype are shown in Figure 6(a) and (b) respectively, where two end-launch connectors are attached to the microstrip feed lines to connect the circuit to the vector network analyzer for the measurement of the scattering parameters.

B. Scattering Parameters

The simulated and measured scattering parameters of the antenna are shown in Figure 7. A good agreement between the simulation and the measured data can be observed. Slight frequency shifts are due to the manufacturing tolerances. Nevertheless, the measured reflection coefficient $|S_{11}|$ at port 1, is equal to −15 dB at 2.4 GHz frequency, while the reflection coefficient $|S_{22}|$ at port 2 is equal to −11 dB at

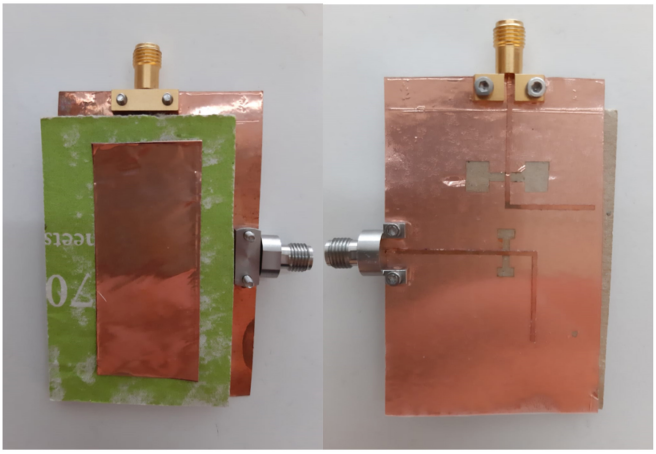

(a) (b)

Fig. 6. Picture of the manufactured antenna prototype, with view from the top side (a) and view from the bottom side (b).

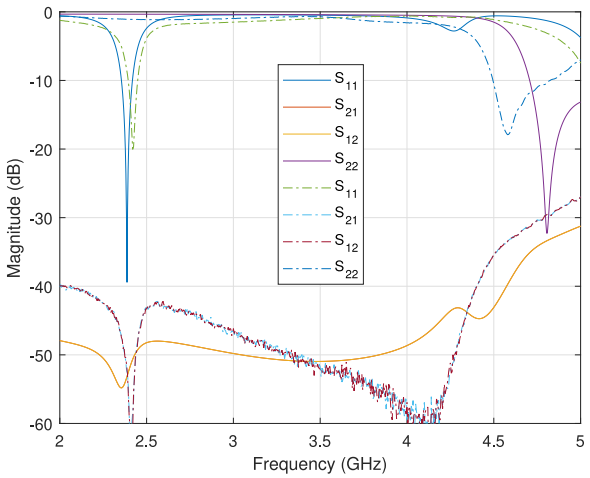

Fig. 7. Antenna scattering parameters. The solid lines correspond to the simulations, and the dashed lines to the measurements.

4.8 GHz, demonstrating a satisfactory antenna matching. The isolation between the ports is also very good, always below −25 dB.

C. Gain and Radiation Pattern

The radiation patterns of the antenna at the two harmonic frequencies are measured and compared to the simulation results. Figure 8 shows an overview of the 3D radiation pattern associated with the two ports of the antenna. The antenna features a radiation efficiency of 53% at f_0 and of 74% at $2f_0$.

Figure 9 shows the radiation patterns on the E and H planes (co-polar components) at 2.4 GHz frequency, associated with Port 1. Figure 10 instead shows the radiation patterns on the E and H planes of the antenna at 4.8 GHz (Port 2). An excellent agreement between simulations and measurements can be noticed. The half power beamwidth for the f_0 antenna is 60 degree on the E plane, and 120 degree on the H plane; the half power beamwidth for the $2f_0$ antenna is 70° for the E plane and 55° on the H plane. The front-to-back ratio is better than 12 dB at both frequencies.

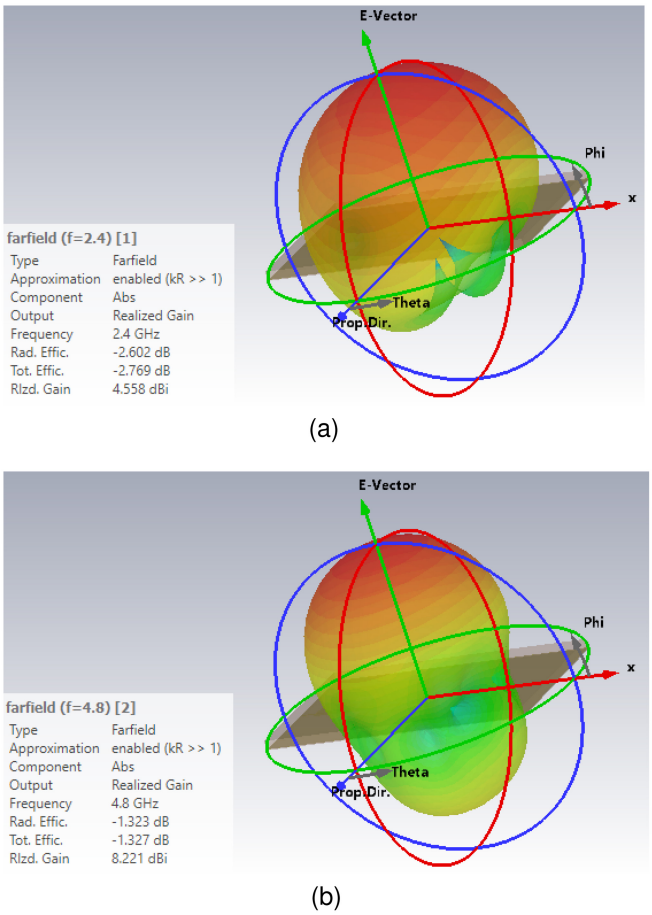

Fig. 8. 3D radiation pattern corresponding to 2.4 GHz (a) and to 4.8 GHz (b).

The antenna's gain was obtained by the direct comparison method, and the results are shown in Figures 11(a) and 11(b). Slight frequency shifts are due again to the manufacturing inaccuracies and uncertainties of the experimental setup. The measured gain at $f_0 = 2.4$ GHz is about 3 dBi, while the gain for the $2f_0$ antenna is about 8.2 dB.

IV. Frequency Doubler Design

The adopted frequency doubler is based on a series-connected Schottky diode and two quarter-wave stubs [15]. The schematic is illustrated in Figure 12 for completeness. The circuit includes also an input and an output matching networks used to achieve input and output impedances of 50 Ω. The output matching network also plays the role of bias tee: the dc component self-generated by the diode has a return through the inductance of the LC matching network. In this way, the dc voltage across the diode is zero, or, equivalently, the diode is zero biased.

The input and output matching networks are designed to minimize the conversion loss CL of the doubler, defined as follows:

$$CL = \frac{P_{in}^{f_0}}{P_{out}^{2f_0}} \tag{1}$$

where $P_{in}^{f_0}$ is the available input power and $P_{out}^{2f_0}$ is the power delivered to the load. To maximize the read range of the tag,

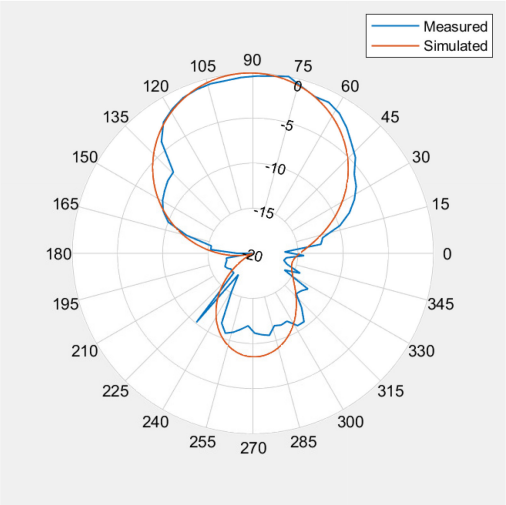

(a)

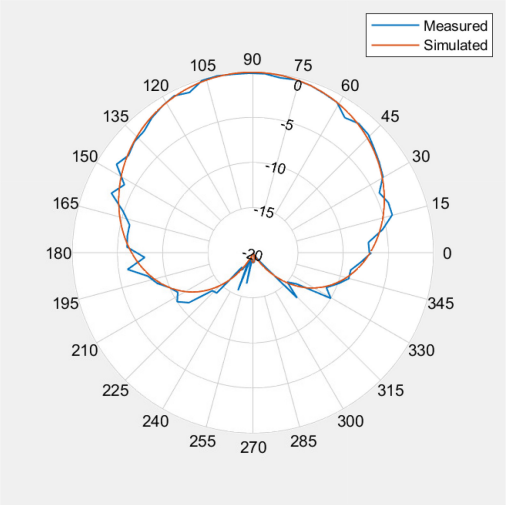

(b)

Fig. 9. 2D radiation patterns of the f_0 antenna at 2.4 GHz. (a) E plane, and (b) H plane.

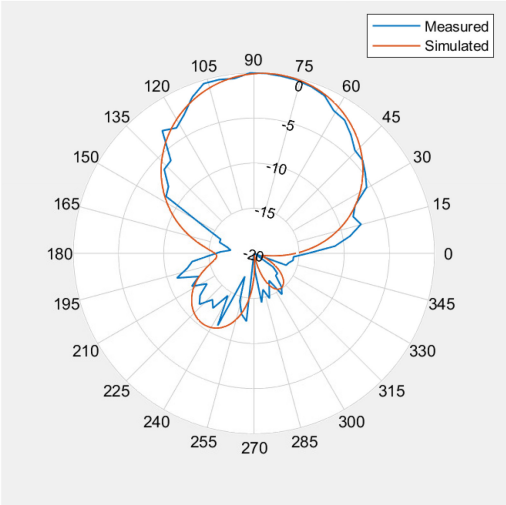

(a)

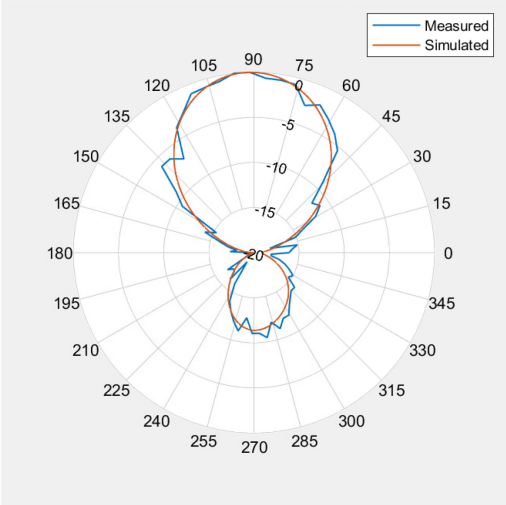

(b)

Fig. 10. 2D radiation patterns of the $2f_0$ antenna at 4.8 GHz. (a) E plane, and (b) H plane.

we need to minimize the conversion loss of the doubler for the available input power corresponding to the sensitivity of the tag.

Assuming the signal propagates in free space, the power received by the reader $P_{RX}^{2f_0}$ when the tag is at a distance R can be estimated using a link budget analysis as follows:

$$P_{RX}^{2f_0} = \frac{1}{4}\frac{P_{tx}^{f_0} G_1^t G_1^r G_2^t G_2^r}{CL}\left(\frac{\lambda_0}{4\pi R}\right)^4 \tag{2}$$

where G_i^j, is the specific antenna gain (i = 1 fundamental, i = 2 2^{nd} harmonic, j = t tag, j = r reader), while λ_0 is the free-space wavelength corresponding to the fundamental frequency. The minimum $P_{RX}^{2f_0}$ that can be detected by the reader corresponds to the sensitivity of the receiver, which in case of harmonic tags is mostly determined by thermal noise.

The frequency doubler is designed using harmonic balance simulations. The design flow is reported in [15]. The simulated conversion loss versus available input power is shown in Figure 13. The minimum CL of the doubler is equal to 13 dB at −10 dBm. For lower available input powers the doubler operates in linear region (CL increases linearly as the available input power decreases). The CL for $P_{in}^{f_0} = -30$ dBm is equal to 27.5 dB.

V. Harmonic Tag

A complete tag is finally manufactured. The three metal layers are manufactured using the copper adhesive laminate technology. Two intermediate steps are shown in Figure 14. In Figure 14(a) the copper adhesive laminate is shown with the desired photoresist patterns (after development in weak soda), while Figure 14(b) shows the layers after wet etching and photoresist removal.

As for the antenna, both the metal layer with the microstrip lines and the ground plane are attached to the two sides of the PLA substrate. Holes are performed in correspondence

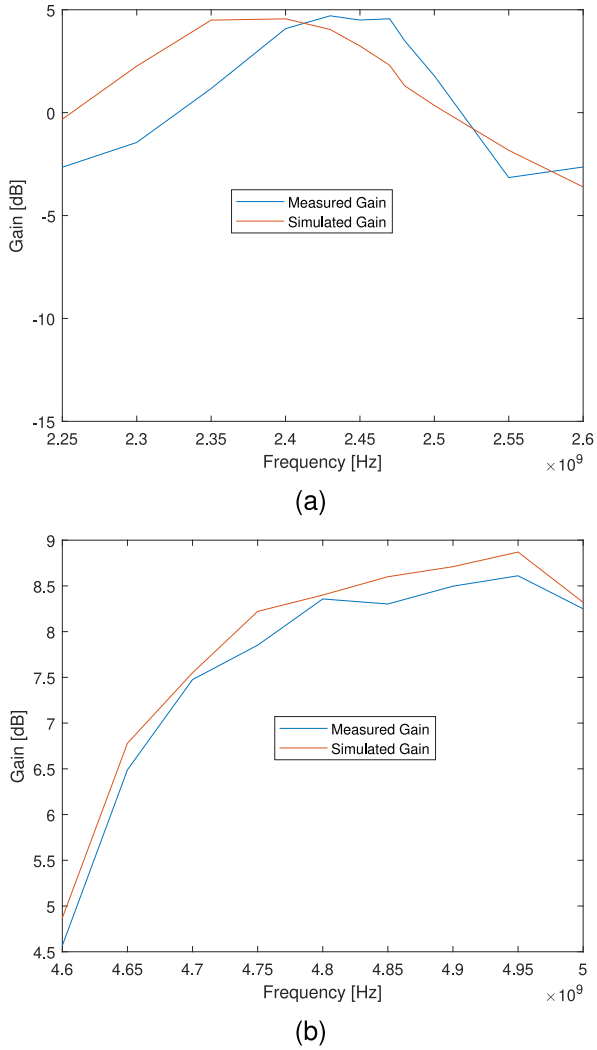

Fig. 11. Gain versus frequency. (a) f_0 antenna port, and (b) $2f_0$ antenna port.

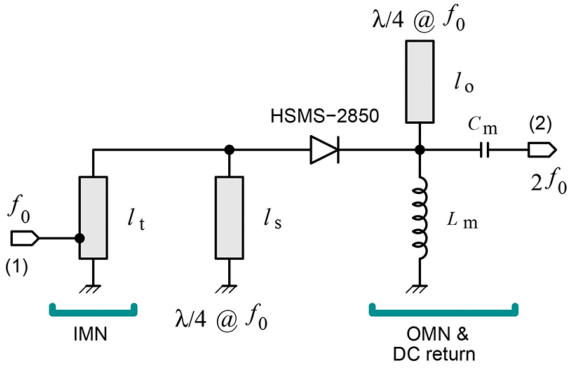

Fig. 12. Schematic of the adopted frequency doubler [15]. The main parameters are: $l_t = 60.4$ mm, $l_s = 21.7$ mm, $l_o = 22$ mm, $C_m = 0.4$ pF, $L_m = 1.6$ nH.

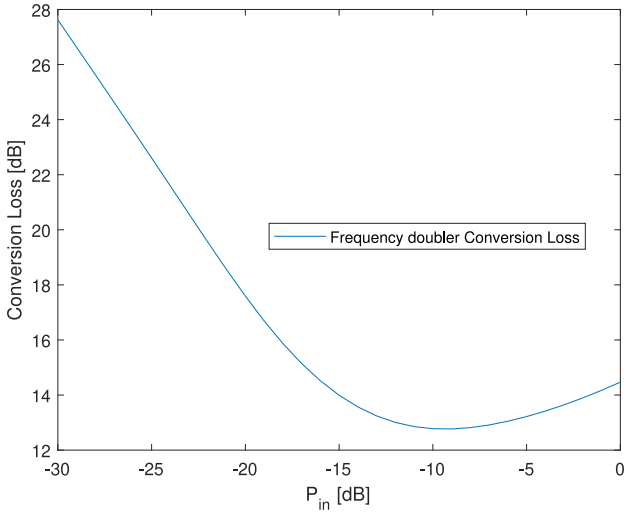

Fig. 13. Frequency doubler conversion-loss as the input power varies.

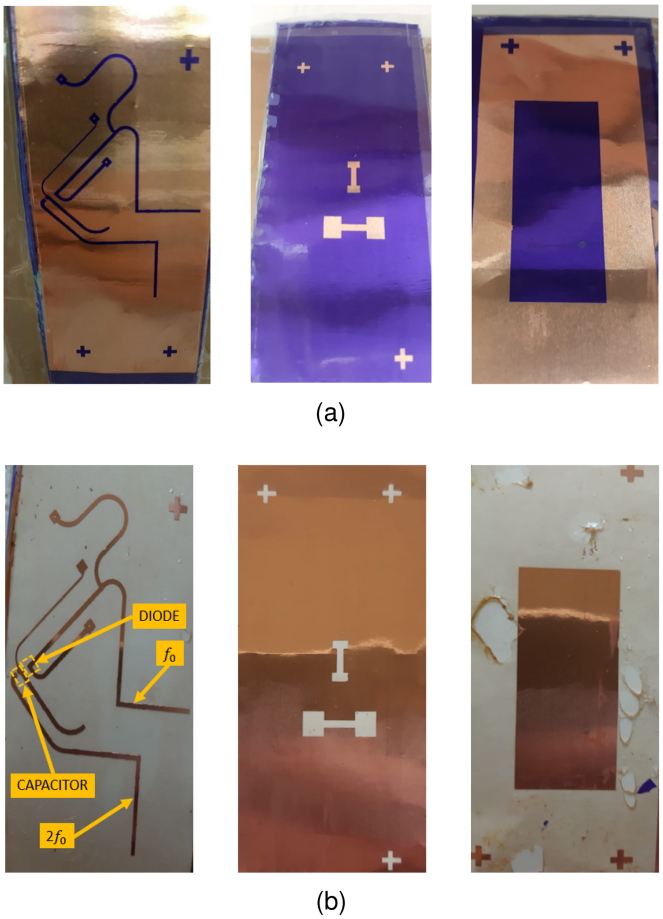

Fig. 14. (a) Picture of the three layers after imprinting the photoresist film with UV light. (b) Photograph of the three layers after acid etching, with removal of the photoresist.

with the vias, which are metalized attaching a piece of copper wire on both metal sides using a colloidal silver paste which solidifies at room temperature. Also, two lumped components, namely the capacitor and the HSMS-2850 Schottky diode, are attached to the frequency doubler microstrip lines using colloidal silver paste. The lines of the frequency doubler are folded to reduce the area occupation of the tag. The rectangular patch instead, is directly attached to the exterior of a parcel made of the same cardboard characterized in Section II-A. Therefore, the circuit on the PLA layer is manufactured separately, it is finally attached to the interior of the parcel, and aligned with the rectangular patch. The tag area is 5×10 cm^2.

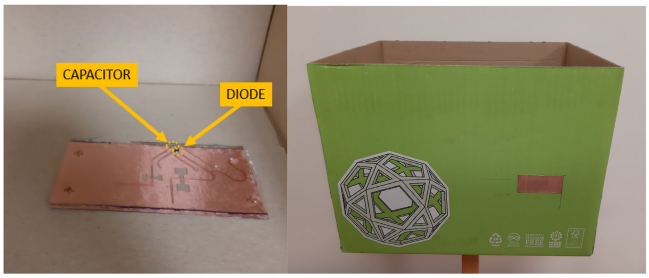

Fig. 15. Panel (a): part of the tag located inside the box, then feed lines and ground slots; panel (b): outside of the box with the patch.

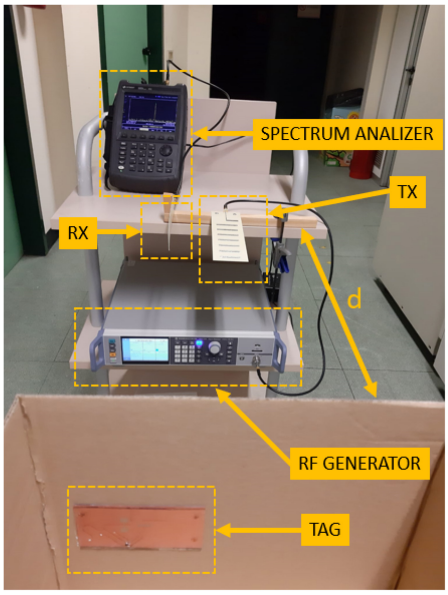

Fig. 16. Tag view. Experimental setup: two yagi uda used for transmission and reception, and harmonic tag placed on the remote box.

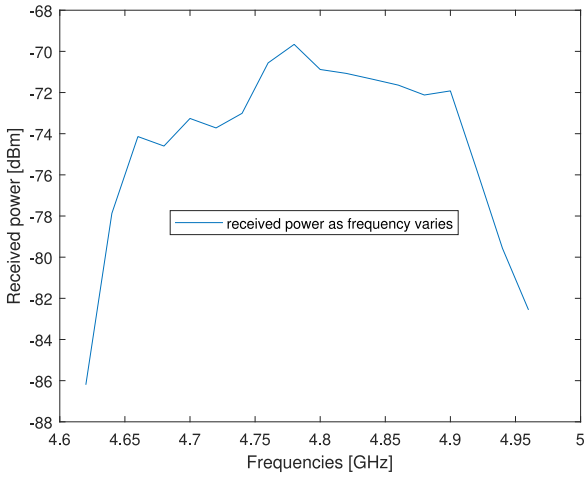

Fig. 17. Power received as the frequency varies, with peak centered on 4.8 GHz.

VI. Experimental Results

The performance of the manufactured proof-of-concept prototype was measured using the setup illustrated in Figure 16. The reader consists of a signal generator connected to a Yagi

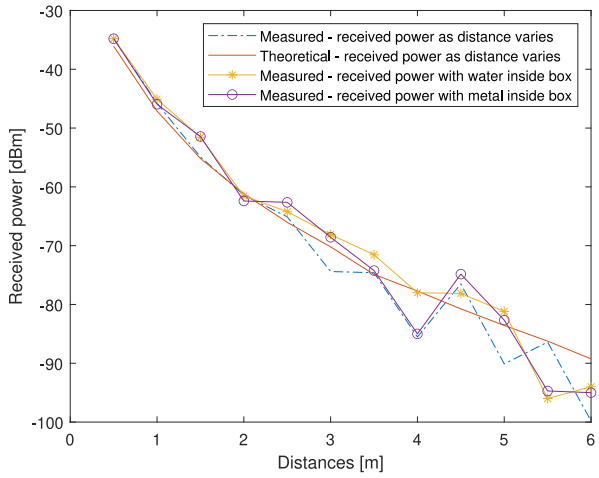

Fig. 18. Received power of second harmonic vs distance. Comparison between theoretical (continuous red) and measured power in different conditions (empty box, water and metal inside the box).

Uda antenna (transmitter side) with an operating frequency of 2.4 GHz; while another Yagi Uda antenna, with operating frequency 4.8 GHz, was connected to the spectrum analyzer, and was used to receive the signal backscattered by the harmonic tag. A stop-band filter is placed between the signal generator and the Yagi-uda antenna to remove the spurious second harmonic generated by the signal generator. The RF transmited power is 15 dBm, which corresponds to 25 dBm EIRP owing to the 10 dBi gain of the Yagi Uda antenna at 2.4 GHz. The gain of the receiving antenna is 14 dBi, and the spectrum analyzer is set to achieve a noise floor of -100 dBm.

The harmonic tag was placed on one side of a cardboard box: the patch antenna exposed on the outside is aligned with the Yagi Uda antennas, while the circuitry including the frequency doubler was placed inside the parcel (see Figure 15).

First, the tag is placed at a fixed distance of 3 m from the reader and the frequency of the transmitter is varied. This study is done to check for eventual frequency shifts in the optimal operating conditions of the tag. The second harmonic power received by the reader versus frequency with the described setup is shown in Figure 17. The maximum received power occurs for 4.8 GHz, thus when transmitting at 2.4 GHz, which corresponds precisely to the design frequency.

Knowing the transmitting antenna gain and the patch receiving gain, it is possible to calculate the input power to the frequency doubler versus distance with the link budget analysis. Then, by comparing the received power with the path loss at $2f_0$ and with the gain of the receiving Yagi-Uda antenna, the conversion loss of the tag can be estimated. By applying this concept to the obtained results at $f_0 = 2.4$ GHz we obtain a conversion loss of 16 dB, in good agreement with the simulation results.

Then, we measured the power of the received second harmonic $P_{rx}^{2f_0}$ versus the tag-to-reader distance (see Figure 18). All measurements are conducted in a laboratory corridor. The obtained results are compared with the theoretical link budget analysis described by (2). Excellent agreement can be noticed for $R < 3$ m. For longer distances, multipath has a higher

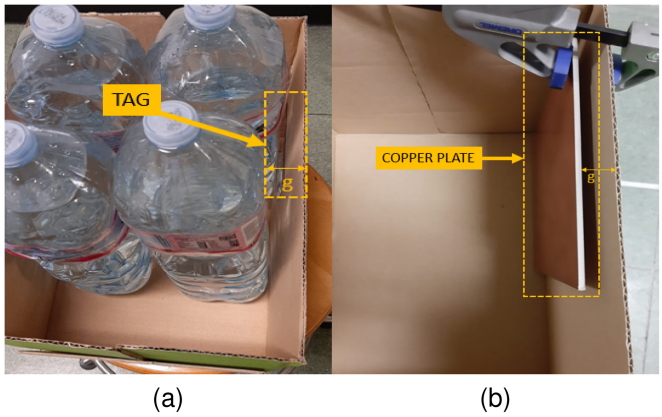

Fig. 19. (a) Tag with water bottles inserted in the box, to test received power at varying distances. (b) Tag with copper plate inserted in box, to test received power at varying distance. The letter g, indicating the gap between the objects and the tag, is 2 mm.

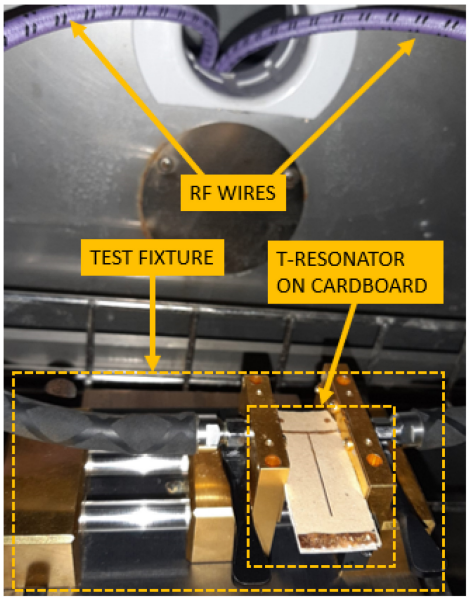

Fig. 20. Picture of cardboard T-resonator characterization in climate chamber.

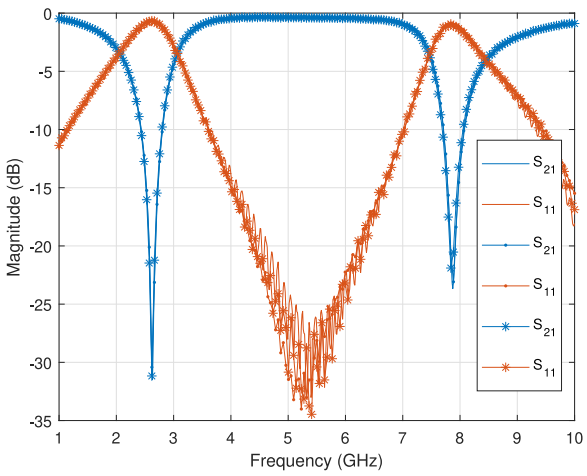

Fig. 21. Scattering parameters of the T-resonator of the PLA material at varying percentages of relative humidity: solid lines indicate values corresponding to a relative humidity of around 50%, lines with circles represent measurements with relative humidity decreased to 30% and lines with stars indicate curves for a humidity of 90%.

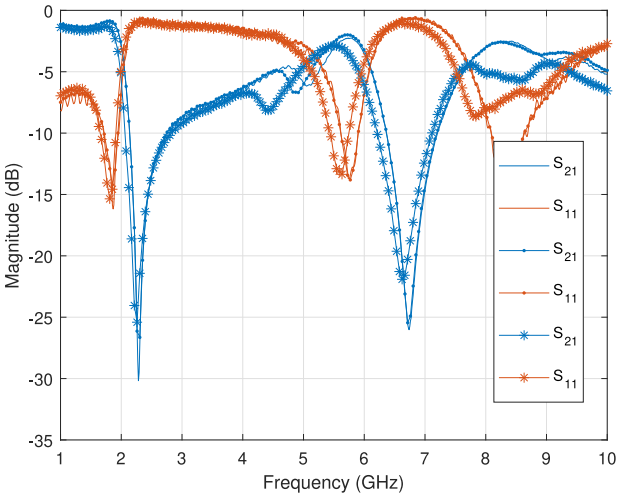

Fig. 22. Scattering parameters of the T-resonator of the cardboard material at varying percentages of relative humidity: solid lines indicate values corresponding to a relative humidity of around 50%, lines with circles represent measurements with relative humidity decreased to 30% and lines with stars indicate curves for a relative humidity of 90%.

impact. Nevertheless, a readout distance of 6 m is obtained. The transmitted power can be increased up to 36 dBm in industrial, scientific and medical (ISM) band. The projected maximum tag-to-reader distance for such a transmitted power is about 15 m.

Finally, the same measurements are repeated with objects inside the box (see Figure 19), such as water and metals. The materials are placed at a distance of 2 mm from the tag (this distance can be guaranteed by adding a protection layer on top of the microstrip line). As shown by Figure 18, the impact of water and metal on the received power is almost negligible and the readout distance remained unchanged.

Furthermore, to verify that the proposed system would maintain its performance under varying environmental conditions, the tag substrates were characterized electromagnetically in a climatic chamber (see Figure 20).

The chamber was first brought to a relative humidity (RH) level of 30% and then to a level of 90%, while the temperature was kept at $20°C$. For both conditions, the scattering parameters of the T-resonators built on top of PLA and cardboard substrates were measured, as shown respectively in Figure 21 and 22. No change in the scattering parameters was found for the PLA, while a small change in the response was detected for the cardboard for RH $=$ 90%, which then resulted in a change in the permittivity of the cardboard, which increases to 1.38.

The antenna was simulated again with the new electromagnetic parameters obtained from the material characterization for RH $=$ 90%. The scattering parameters of the antenna remained substantially unchanged, as can be seen from Figure 23, and the broadside gain with the radiation pattern also proved to be robust to changes in relative humidity, as

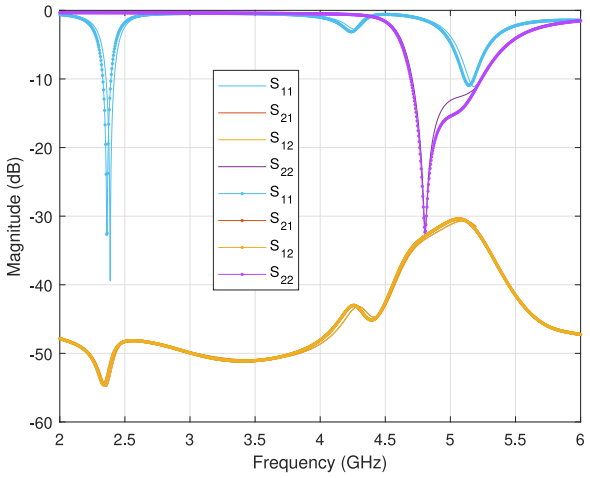

Fig. 23. Scattering parameters of the antenna with different relative humidity: the solid line corresponds to RH = 50%, while the dotted line corresponds to RH = 90%.

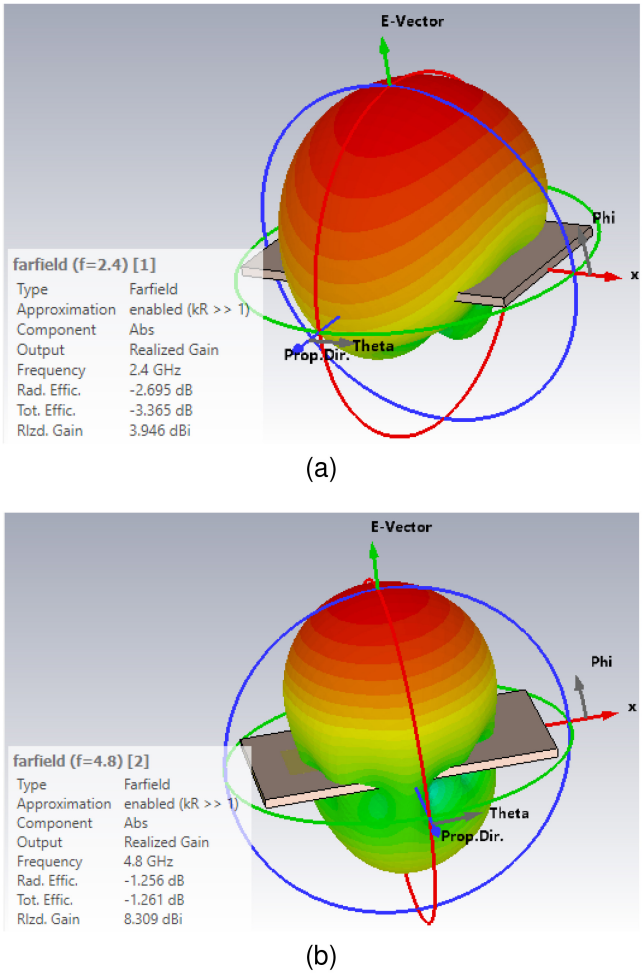

Fig. 24. 3D radiation pattern corresponding to 2.4 GHz (a) and to 4.8 GHz (b), at 90% humidity.

shown in Figure 24. The limited variation is due to the fact that the adopted cardboard substrate is actually mostly made of air due to the large amount of voids.

VII. Conclusion

A compact harmonic tag, robust to water and metal detuning, has been presented. The tag consists of three metal layers and it is manufactured on organic substrates to reduce its environmental impact and improve the tag integrability in parcels and packages of interest. A complete tag fully integrated in a parcel has been presented. The tag has demonstrated to be able to reach the remarkable readout distance of 6 m with a transmitter power of 25 dBm EIRP. The readout distance remained unchanged when metal or water objects are placed in close proximity with the tag, thereby proving the robustness of the proposed approach. The proposed tag is one-bit and can be used only for tracking applications. However, strategies to introduce multi-bit information have been studied, for instance by adding a modulation port, as reported in [15] and [16], and will be implemented in the future.

References

[1] A. Boaventura, J. Santos, A. Oliveira, and N. B. Carvalho, "Perfect isolation: Dealing with self-jamming in passive RFID systems," *IEEE Microw. Mag.*, vol. 17, no. 11, pp. 20–39, Nov. 2016.

[2] M. Lach, M. Hani, C. Looschen, C. Buchberger, and E. Biebl, "Evaluation of UHF-RFID tag performance considering near-field and detuning effects on various dielectric and inhomogeneous application surfaces," in *Proc. Kleinheubach Conf.*, 2021, pp. 1–4.

[3] L. H. Mei, W. J. Yue, X. L. Kun, and Y. T. Xin, "Influence of UHF tags in the different material surface to RFID system," in *Proc. 3rd Asia-Pac. Conf. Antennas Propagat.*, 2014, pp. 713–715.

[4] J. Zhu, Y. Li, C. Jin, X. Liu, and H. Liu, "Optimum separation for performance improvement of RFID solenoid coil antenna in metallic environments," *IEEE Antennas Wireless Propag. Lett.*, vol. 20, no. 9, pp. 1611–1615, Sep. 2021.

[5] N. Faudzi, M. Ali, I. Ismail, H. Jumaat, and N. Sukaimi, "Compact microstrip patch UHF-RFID tag antenna for metal object," in *Proc. IEEE Symp. Wireless Technol. Appl. (ISWTA)*, 2014, pp. 160–164.

[6] B. Li, Y. He, L. Zuo, and Y. Long, "Metric of the application environment impact to the passive UHF RFID system," *IEEE Trans. Instrum. Meas.*, vol. 63, no. 10, pp. 2387–2395, Oct. 2014.

[7] B. G. Colpitts and G. Boiteau, "Harmonic radar transceiver design: Miniature tags for insect tracking," *IEEE Trans. Antennas Propag.*, vol. 52, no. 11, pp. 2825–2832, Nov. 2004.

[8] "The RECCO system." Accessed: Jun. 20, 2022. [Online]. Available: http://www.recco.com/the-recco-system

[9] V. Palazzi, F. Alimenti, C. Kalialakis, P. Mezzanotte, A. Georgiadis, and L. Roselli, "Highly integrable paper-based harmonic transponder for low-power and long-range IoT applications," *IEEE Antennas Wireless Propag. Lett.*, vol. 16, pp. 3196–3199, 2017.

[10] K. Rasilainen, J. Ilvonen, A. Lehtovuori, J. M. Hannula, and V. Viikari, "On design and evaluation of harmonic transponders," *IEEE Trans. Antennas Propag.*, vol. 63, no. 1, pp. 15–23, Jan. 2015.

[11] X. Gu, N. N. Srinaga, L. Guo, S. Hemour, and K. Wu, "Diplexer-based fully passive harmonic transponder for sub-6-GHz 5G-compatible IoT applications," *IEEE Trans. Microw. Theory Techn.*, vol. 67, no. 5, pp. 1675–1687, May 2019.

[12] V. Palazzi, L. Balocchi, S. Bonafoni, and L. Roselli, "Slot-fed dual-port patch antenna for compact harmonic transponders," in *Proc. IEEE 12th Int. Conf. RFID Technol. Appl. (RFID-TA)*, Sep. 2022, pp. 86–89.

[13] V. Palazzi, S. Bonafoni, F. Alimenti, P. Mezzanotte, and L. Roselli, "Feeding the world with microwaves: How remote and wireless sensing can help precision agriculture," *IEEE Microw. Mag.*, vol. 20, no. 12, pp. 72–86, Dec. 2019.

[14] V. Palazzi, F. Alimenti, D. Zito, P. Mezzanotte, and L. Roselli, "A 24-GHz single-transistor oscillator on paper," *IEEE Microw. Compon. Lett.*, vol. 30, no. 11, pp. 1085–1088, Nov. 2020.

[15] V. Palazzi et al., "Low-power frequency doubler in cellulose-based materials for harmonic RFID applications," *IEEE Microw. Compon. Lett.*, vol. 24, no. 12, pp. 896–898, Dec. 2014.
[16] V. Palazzi, L. Roselli, M. M. Tentzeris, P. Mezzanotte, and F. Alimenti, "Energy-efficient harmonic transponder based on on-off keying modulation for both identification and sensing," *Sensors*, vol. 22, no. 2, p. 620, 2022.

Leonardo Balocchi received the M.S. degree (magna cum laude) in electrical engineering from the University of Perugia, Italy, in 2021. His research interests include distributed sensing and RFID transponders.

Valentina Palazzi (Member, IEEE) received the M.S. degree in electrical engineering and the Ph.D. degree in industrial and information engineering from the University of Perugia, Italy, in 2014 and 2018, respectively.

In 2015, she was a Visiting Ph.D. student with the Tyndall National Institute, Cork, Ireland. In 2016, she did a short-term scientific mission with the Centre Tecnològic de Telecomunicacions de Catalunya, Barcelona, Spain, sponsored by the cost action IC1301 "WiPE." From December 2016 to April 2017, she was a Student Intern with the Agile Technologies for High-Performance Electromagnetic Novel Applications Research Group, School of Electrical and Computer Engineering, Georgia Institute of Technology, Atlanta, GA, USA. Since 2019, she has been a Researcher with the High Frequency Electronics Laboratory, Department of Engineering, University of Perugia, Italy. She has coauthored more than 60 articles, and holds three patents. Her current research interests include the design of RF components, wireless sensors, radar front ends, wireless power transfer technologies, additive manufacturing processes, and conformal electronics.

Dr. Palazzi was a recipient of the First Place Award of the Student Design Competition on Wireless Energy Harvesting at the 2016 IEEE MTT-S "International Microwave Symposium" (IMS), the IEEE MTT-S Graduate Fellowship in 2017, the 2017 MTT-S Prize—Italy Chapter Central and Southern Italy, the URSI Young Scientist Best Paper Award conferred at the 2019 URSI Italian National Meeting, the Second Place at the 3 Minute Thesis Competition held at IMS 2021, and the GAAS Young Scientist Recognition (URSI Commission D) at GASS 2021. She is the 2023 Microwave Theory and Technology Society (MTT-S) AdCom Secretary. She is the Chair of the IEEE MTT-S Technical Committee-26 RFID, Wireless Sensor and IoT, and the Early Career Representative of the Commission D "Electronics and Photonics" of the International Union of Radio Science (URSI).

Stefania Bonafoni (Member, IEEE) received the Laurea (magna cum laude) and Ph.D. degrees in electronic engineering from the University of Perugia, Perugia, Italy, in 1997 and 2000, respectively. Since 2005, she has been with the Department of Engineering, University of Perugia, where she teaches the class of remote sensing. Her research interests include retrieval of geophysical parameters from ground- and space-based sensors (by microwave and infrared radiometry and by GPS), microwave propagation studies in the atmosphere (models and applications), and sensor data analysis for Earth Observation.

Federico Alimenti (Senior Member, IEEE) received the Laurea degree (magna cum laude) and Ph.D. degrees in electronic engineering from the University of Perugia, Italy, in 1993 and 1997, respectively. He was a Visiting Scientist with the Technical University of Munich, Germany. Since 2001, he has been with the Department of Engineering, University of Perugia, teaching the class of RFIC Design. From 2011 to 2014, he was the Scientific Coordinator of the ENIAC ARTEMOS Project. In Summer 2014, he was a Visiting Professor with EPFL, Switzerland. He has participated at the Summer School 2017, held at Infineon Austria AG, Villach, as a Keynote lecturer. In 2018, he got the qualification as a Full Professor. He has authored a European Patent (EP2660755) and more than 200 papers in journals conferences and books. The H-index of Federico Alimenti is 20 with more than 1500 citations (source Scopus); 23 with more than 2000 citations (source Google Scholar). His interests are about microwave and RFIC design. In 1996, he was a recipient of the URSI Young Scientist Award. In 2013, he was the recipient of the IET Premium (Best Paper) Award and the TPC Chair of the IEEE Wireless Power Transfer Conference. He won the "Mario Sannino" Award for the best research in the field of microwave electronics.

Paolo Mezzanotte (Member, IEEE) was born in Perugia, Italy, in 1965. He received the Ph.D. degree from the University of Perugia, Perugia, in 1997. Since 2007, he has been an Associate Professor with the University of Perugia, where he has been involved in teaching the classes "Radio-frequencies Engineering" and "Systems and Circuits for IoT." He was the Vice Head of the Department of Engineering, University of Perugia from 2014 to 2019. These research activities are testified by over 170 publications in the most reputed specialized journals and at the main conferences of the microwave scientific community. His present H-index is 22 (source Scopus). His current research interests include the development of microwave circuits on bio-compatible substrates and the enabling technologies for IoT. He served as the Chair of the IEEE Technical Committee MTT-24-RFID Technologies for the biennium from 2018 to 2019. He is the Chair of the IEEE Topical Conference on Wireless Sensors and Sensor Networks and an Associate Editor of *Applied Computational Electromagnetics Society Journal* and IEEE JOURNAL OF MICROWAVES.

Luca Roselli (Fellow, IEEE) joined the University of Perugia, Perugia, Italy, in 1991. In 2000, he founded the spin-off WiS Srl. He is currently a Qualified Full Professor with the University of Perugia, where he teaches applied electronics and coordinates the High Frequency Electronics Laboratory. He has authored over 280 papers (H-i 23, i10 51, over 2200 citations-Scholar) and *Green RFID System* (Cambridge Univ. Press, 2014). He was involved in electronic technologies for Internet of Things for six years. His current research interests include HF electronic systems with a special attention to RFID, new materials, and wireless power transfer.

Mr. Roselli is the Co-Chair of the IEEE Wireless Sensor Network Conference. He organized the VII Computational Electromagnetic Time Domain in 2007 and the first IEEE Wireless Power Transfer Conference in 2013. He is an Associate Editor of *IEEE Microwave Magazine*. He is involved on the boards of several international conferences. He is a Reviewer for many international reviews, including the PROCEEDINGS OF THE IEEE, the IEEE TRANSACTIONS ON MICROWAVE THEORY AND TECHNIQUES, and IEEE MICROWAVE AND WIRELESS COMPONENTS LETTERS. He was a member of the Board of Directors of ART Srl, Urbino, Italy, from 2008 to 2012. He is a member of the list of experts of the Italian Ministry of Research, the past Chair of the IEEE Technical Committees MTT-24-RFID, the Vice Chair of 25-RF Nanotechnologies, 26-Wireless Power Transfer, the ERC Panel PE7, the Advisory Committee of the IEEE-WPTC, and the Chairman of the SC-32 of IMS.

Open Access funding provided by 'Università degli Studi di Perugia' within the CRUI CARE Agreement